Time-Domain Simulation for Voltage Collapse Prediction and Wide-Area Control

Z. Shahooei, B. A. Mork, M. Kavimandan, L. J. Bohmann

***Abstract*--This paper proposes and develops an EMTP-based time-domain approach for voltage collapse simulation. Power-voltage (P-V) curves have been used extensively to analyze voltage stability with respect to active power demand. Most methods found in literature use steady-state power-flow analysis for predicting voltage collapse. Static approaches use linearized equations and the Jacobian matrix of the system for analysis of voltage collapse. Using conventional methods, nonlinearities and resultant harmonics are not addressed, nor are frequency-dependencies or natural responses to step-changes in the system. In general, power system is nonlinear, frequency dependent, and time-varying. Most especially, voltage collapse is a nonlinear phenomenon as a result of constant changes in power system, load dynamics, nonlinearities such as transformers and FACTS devices, and control strategies. Different load models which can be slowly ramped have been developed in EMTP/ATP to conduct time-domain simulations. Then P-V curves are plotted and traced by varying the load impedance in time-domain. The simulations are carried out and verified for both dc and ac systems, comparing to both continuous power flow methods and dynamic equations of the system.**

***Keywords*: Dynamic Instability, P-V Curve, Time-Domain Simulation, Voltage Collapse, Voltage Stability**

I. Introduction

THE economic and environmental considerations force the system to operate near its stability limits and this may increases the risk of angle and voltage instability following a disturbance. According to definition and classification of Power system stability By IEEE/CIGRE, Voltage stability refers to the ability of a power system to maintain steady voltages at all buses in the system after being subjected to a disturbance from a given initial operating condition [1].

Voltage instability is an evolving problem; the dynamic changes of power system and subsequent cascading contingencies after the disturbance are the main causes of voltage instability. Furthermore, utilizing Flexible AC Transmission System (FACTS) devices, emerging of independent power producers, and competitive environment of power system make the power system more complex to control and also more vulnerable to disturbances.

Disturbances, both large and small, may lead to voltage collapse. Large disturbances include loss of a generator, a transmission line, or a transformer. Small disturbances include variation of load, and temporary faults. The event can take place within a time frame of fractions of a second to several seconds and minutes.

Voltage collapse is considered a dynamic process; however, because of large system size and process time of algebraic and differential equations, many methods found in literature use static (steady-state) analysis for predicting voltage collapse. Static analysis takes a snapshot of the system at a particular instant of time and gives an indication of the whole system stability. At each of the snapshots of the system, the overall system equations reduces to algebraic equations. Then the linearized equations found for each operating point based on power-flow is as below [2].

$$\begin{bmatrix}\Delta P\\ \Delta Q\end{bmatrix}=\begin{bmatrix}\frac{\partial P}{\partial \theta} & \frac{\partial P}{\partial V}\\ \frac{\partial Q}{\partial \theta} & \frac{\partial Q}{\partial V}\end{bmatrix}\begin{bmatrix}\Delta \theta\\ \Delta V\end{bmatrix} \tag{1}$$

Where ΔP, ΔQ are the mismatch active and reactive power vectors; and ΔV, $\Delta \theta$ are the voltage magnitude and angle change vectors.

$$J=\begin{bmatrix}\frac{\partial P}{\partial \theta} & \frac{\partial P}{\partial V}\\ \frac{\partial Q}{\partial \theta} & \frac{\partial Q}{\partial V}\end{bmatrix} \tag{2}$$

J is the Jacobian matrix of partial derivative and its elements give the relationship between the small changes in bus voltage with changes in active and reactive power. Static approaches use the Jacobian matrix for analysis of voltage collapse. In [2] it is shown in detail that at the point of voltage collapse, the power-flow Jacobian matrix becomes singular. Relying on the power flow Jacobian makes it difficult to include time-varying effects, such as synchronous machines' emergency reactive power limits, or nonlinear effects, such as transformer saturation.

Power-voltage (P-V) curves have been used extensively to

Z. Shahooei is with Department of Electrical and Computer Engineering, Michigan technological University, Houghton, MI 49931 USA (zshahooe@mtu.edu)

B. A. Mork is with Department of Electrical and Computer Engineering, Michigan technological University, Houghton, MI 49931 USA (bamork@mtu.edu)

M. Kavimandan is with Black & Veatch, Raleigh, NC, USA (KavimandanM@bv.com).

L.J. Bohmann is with Department of Electrical and Computer Engineering, Michigan technological University, Houghton, MI 49931 USA (ljbohman@mtu.edu)

Paper submitted to the International Conference on Power Systems Transients (IPST2015) in Cavtat, Croatia June 15-18, 2015

analyze voltage stability with respect to active power demand. The general approach used to generate P-V curves is to run continuous power flow simulations increasing the load at a particular bus in an area while keeping the load power factor constant. This method relies on phasor analysis, which ignores frequencies other than the synchronous frequency. Thus, nonlinearities and resultant harmonics are not addressed, nor are frequency-dependencies or natural responses to step-changes in the system.

The proposed methods in the literature which investigate voltage stability typically include one or a combination of the steady-state methods mentioned before. Reference [3] uses a wide-area measurement system based on PMU data to get a dynamic model of the power system; then the equilibrium of this model is determined without a time-domain simulation. The system is stable if an equilibrium exists. In [4] the authors focus on online voltage security assessment based on the voltage stability margin. Their method is based on predicting different scenarios for load and generation variations and making a database of different operation points using continuous power flow method. Reference [5] uses the Fast Time Domain (FTD) simulation to analyze different contingencies. Then a participation factor is defined for each load and generator based on modal analysis and based on these participation factors a priority list is developed to re-dispatch the active power and minimize load shedding. in [6] a voltage stability index is developed based on the transferred power from each transmission line and the transmission line capacity. Then this index is used as a constraint in Optimal Power Flow (OPF) problem to improve voltage stability. Many other methods found in literature [7]-[12] use static analysis for predicting voltage collapse.

The conventional voltage stability analysis methods merely rely on phasor analysis and power flow. This means that in these methods we neglect the frequencies other than fundamental frequency. If we model the power system components in time-domain, we can consider the nonlinearity, frequency dependency and also transient effects on voltage stability. Since most of the control actions have nonlinear effects on the power system, time-domain modeling will help us to take appropriate control actions and monitor their accurate effects. The transient behavior of the system could be captured more precisely if the variable loads are modeled in time-domain. For example, in bifurcation simulation to analyze different types of ferroresonant responses, the capacitance connected to the ferroresonant phase is slowly ramped to plot voltage vs. capacitance [13]. Reference [14] presents a method to model time-varying capacitance in ATP.

In this paper, an EMTP-based time-domain approach is developed for voltage collapse simulation. Load models which can be slowly ramped are developed in EMTP/ATP to conduct time domain simulations. The load models include time-variant resistive, inductive, and capacitive loads. The MODELS language within EMTP/ATP has been used. Different load blocks can be combined to define the load level, power factor, and aggregate nature of the load. Then, P-V curves have been plotted and traced by varying the load impedance in time-domain using EMTP/ATP. Then this method is benchmarked against traditional phasor-based methods. The simulations are carried out and verified for both dc and ac systems, comparing to both continuous power flow methods and dynamic equations of the system.

The paper is divided in seven sections. Section II describes background details of the P-V curve. Section III gives implementation details for different time-varying load models. Section IV presents the network modeling and DC system studies. Section V includes the results of time-domain simulations for AC systems. In section VI the results obtained from developed models are validated against conventional steady-state methods. Finally, conclusions drawn from this work are discussed in section VII.

II. Background

One of the widely used methods of illustrating voltage collapse is based on the relationship between the transmitted power and receiving voltage. With this method we can find the available power margin before the voltage collapse point. This is shown as a plot of voltage vs. active power for loads with different power factors. In a two bus system, assume that the generator voltage is $V_1\angle\theta_1$, the load bus voltage is $V_2\angle\theta_2$, and the transmission line admittance is $Y = G + jB$. Then the active and reactive power delivered to the load is:

$$P_D = |V_1||V_2|G\cos(\theta_1-\theta_2) - |V_2|^2 G - |V_1||V_2|B\sin(\theta_1-\theta_2) \quad (3)$$

$$Q_D = |V_2|^2 B - |V_1||V_2|B\cos(\theta_1-\theta_2) - |V_1||V_2|G\sin(\theta_1-\theta_2) \quad (4)$$

If we assume G=0, then:

$$P_D = -|V_1||V_2|B\sin(\theta_1-\theta_2) \quad (5)$$

$$Q_D = |V_2|^2 B - |V_1||V_2|B\cos(\theta_1-\theta_2) \quad (6)$$

The Complex power delivered to load is:

$$S_D = |V||I|(\cos\theta + j\sin\theta) = P_D(1 + \mathrm{j}\tan\theta) \quad (7)$$

If $\beta = \tan\theta$; now we square both equations (3), (4) and add them together; then we will have:

$$P_D{}^2 + \left(P_D\beta + |V_2|^2 B\right)^2 = |V_1|^2|V_2|^2 B^2\left(\sin^2\theta + \cos^2\theta\right) \quad (8)$$

$$P_D{}^2 + \left(P_D\beta + |V_2|^2 B\right)^2 = |V_1|^2|V_2|^2 B^2 \quad (9)$$

Dividing the above equation by B^2 and finding $|V_2|^2$ based on the other parameters will lead to the below equation:

$$\left(|V_2|^2\right)^2+\left[\frac{2P_D\beta}{B}-|V_1|^2\right]|V_2|^2+\frac{P_D^2}{B^2}\left(1+\beta^2\right)=0 \tag{10}$$

(10) is a quadratic equation and if we solve it for variable $|V_2|^2$, then:

$$|V_2|^2=\frac{|V_1|^2}{2}-\frac{P_D\beta}{B}\pm\sqrt{\left[\frac{|V_1|^4}{4}-\frac{P_D}{B}\left(\frac{P_D}{B}+\beta|V_1|^2\right)\right]} \tag{11}$$

If we plot this equation, it is called a P-V curve which is shown in Fig. 1 [15].

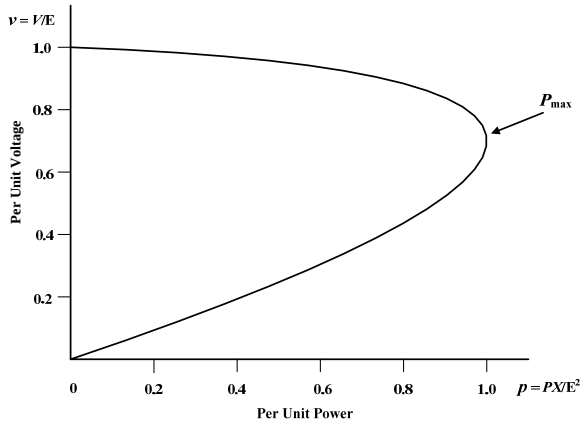

Fig. 1. Normalized P-V curve [15]

P-V curve analysis involves conducting a series of power flow solutions for increasing load power while we are monitoring the voltage. The general approach is to run power flow simulations; increasing the load at a particular while keeping the power factor constant. The curve shown in Fig. 1 is also termed as "nose" curve. The region above the "nose" point is considered to be stable while the region below is unstable.

In this paper the P-V curves are developed based on time-domain analysis using actual voltage waveforms and instantaneous power by varying the load impedance in real time. The accuracy of this method is verified by comparing the results with continuous power flow simulation and also mathematical power flow equations.

III. Time-domain Load Models

In this paper, the power system is modeled in the most detailed format using time-domain method. Built into EMTP/ATP is TACS (Transient Analysis of Control System) for modeling controls [16]. The MODELS language within EMTP/ATP has been used in which the users are able to write their own procedures [17]. Three different load models are developed in ATPDraw to simulate time-varying resistive, inductive and capacitive loads. Using these load models, any time-varying load with desired power factor can be simulated.

A. Time-varying resistive load

In this model we specify the maximum and minimum value of the resistance and from these limits, the slope of the resistance is calculated. Then the value of the resistance is decreased linearly in each time step starting from the maximum value.

$$R\left(t+\Delta t\right)=R_{initial}+\left[\left(t+\Delta t\right)\times slope\right] \tag{12}$$

t is time of simulation and Δt is time step.

The ATPDraw model is shown in Fig. 2 and it includes a TACS controlled resistor type 91 and a MODELS block.

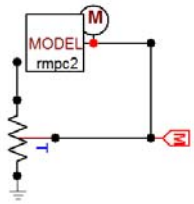

Fig. 2. Time-varying resistor model

B. Time-varying inductive load

Time-varying magnetic flux induces a voltage across the inductor. (13) And (14) show the induced voltage (v_l) and magnetic flux (ϕ) of an inductor (L).

$$v_l=\frac{d\phi}{dt} \tag{13}$$

$$\phi=L\,i \tag{14}$$

If we assume that the inductor is changing linearly and decreasing from its initial value (L_0) to its final value (L_{end}); then in each time step (t) the inductance value is:

$$L\left(t\right)=L_0+Kt \tag{15}$$

K is the changing rate of the inductance. We can model a time-varying inductance using a Norton current source and an equivalent conductance. Since (L)is time-varying, we cannot take it out from the derivative. $k-1$ and k are two consecutive time steps. Using partial derivative and trapezoid rule to approximate the integral, then:

$$v_l=\frac{\partial L\,i}{\partial t}\Rightarrow\int_{k-1}^{k}v_l\,dt=\int_{k-1}^{k}\partial L\,i \tag{16}$$

$$\frac{v_{l,k}+v_{l,k-1}}{2}\Delta t=L_k i_k-L_{k-1}i_{k-1} \tag{17}$$

$$L_k i_k=L_{k-1}i_{k-1}+\frac{v_{l,k}+v_{l,k-1}}{2}\Delta t \tag{18}$$

$$i_k=\left(\frac{L_{k-1}}{L_k}i_{k-1}+v_{l,k-1}\frac{\Delta t}{2L_k}\right)+v_{l,k}\frac{\Delta t}{2L_k} \tag{19}$$

The equivalent circuit is shown in Fig. 3; and the Norton current source and the conductance would be:

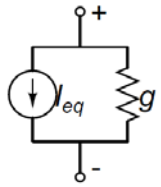

Fig. 3. Inductance equivalent circuit

$$i_{eq} = \left(\frac{L_{k-1}}{L_k} i_{k-1} + v_{l,k-1} \frac{\Delta t}{2 L_k} \right) \tag{20}$$

$$g_k = \frac{\Delta t}{2 L_k} \tag{21}$$

$$i_k = i_{eq} + g_k . v \tag{22}$$

The component model includes a type 94 Norton source MODELS block and it is shown in Fig. 4.

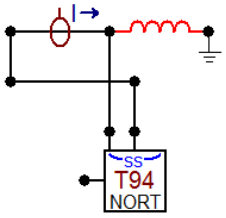

Fig. 4. Time-varying inductor model

C. Time-varying capacitive load

When there is a voltage difference across a capacitor, an electric field develops; causing a current flow through the capacitor. The variable capacitor value changes linearly and it increases from its initial value (C_0) to its final value (C_{end}). So the capacitor value at each time step $C(t)$ would be:

$$C(t) = C_0 + kt \tag{23}$$

The current (i) flowing through capacitor (C) while voltage across the capacitor is v:

$$i = \frac{\partial Cv}{\partial t} \tag{24}$$

As it is shown in Fig. 5, we can develop an equivalent Norton current source and a resistance to model time-varying capacitor. Again, $k-1$ and k are two consecutive time steps.

$$i_c = \frac{\partial Cv}{\partial t} \Rightarrow \int_{k-1}^{k} i_c \, dt = \int_{k-1}^{k} \partial Cv \tag{25}$$

$$\frac{i_{c,k} + i_{c,k-1}}{2} \Delta t = C_k v_k - C_{k-1} v_{k-1} \tag{26}$$

$$i_{c,k} \frac{\Delta t}{2} = C_k v_k - C_{k-1} v_{k-1} - i_{c,k-1} \frac{\Delta t}{2} \tag{27}$$

$$i_{c,k} = v_k \frac{2C_k}{\Delta t} - \left(\frac{2C_{k-1}}{\Delta t} v_{k-1} + i_{c,k-1} \right) \tag{28}$$

$$R_{eq,k} = \frac{\Delta t}{2C_k} \tag{29}$$

$$I_{inj} = \frac{2C_{k-1}}{\Delta t} v_{k-1} + i_{c,k-1} \tag{30}$$

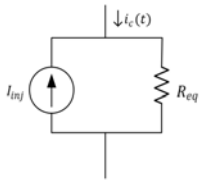

Fig. 5. Capacitor equivalent circuit

The capacitor model is shown in Fig. 6 and it includes two TACS controlled current sources, a TACS controlled resistor and a MODELS block.

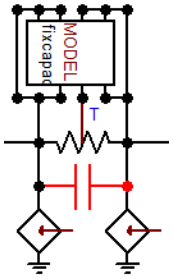

Fig. 6. Time-varying capacitor model

D. Time-varying Loads with desired PF

To simulating leading and lagging loads, we can model a time-varying load with any specific desired power factor using different models developed for time-varying resistive, inductive, and capacitive loads. The important point is that the rate of change of active and passive parts of the load in time needs to be in a way that the power factor remains constant.

IV. Network Modeling

Time-domain models of sample systems are developed in EMTP/ATP to demonstrate time-domain method capability for analyzing voltage stability. In this section modeling of dc and ac power systems are described in detail.

A. Transmission line

In this work, we have modeled transmission line as series RL branch. The lumped capacitance at both ends is neglected.

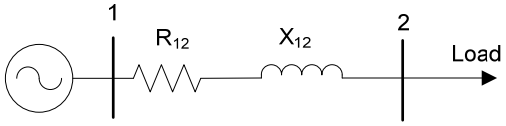

Fig. 7. One line diagram for sample system

The corresponding transmission line representation in ATP

is shown in Fig. 8. Line performance equation is as (31).

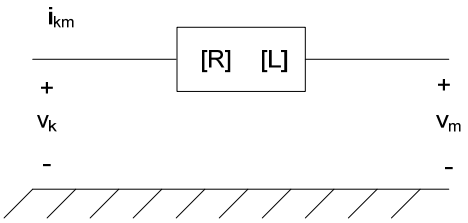

Fig. 8. Transmission line model in ATP

$$v_k - v_m = [L]\frac{di_{km}}{dt} + [R]i_{km} \tag{31}$$

B. DC system

A simple dc system is shown in Fig. 9. The complete analysis of this system is published in [18]. Therefore, it is a starting point to verify the results obtained from EMTP/ATP models. Details of system are: E = 1 V, $r_{branch} = 0.5\Omega$, and R_{load} is variable. To trace a P-V curve for this system, R_{load} is varied according to (12). For different values of R_{load}, there is a corresponding power flowing into bus 2.

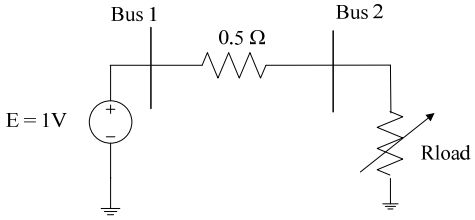

Fig. 9. 2 bus dc system [1]

To capture the details in simulations, the step size is selected as 50µs. The value of resistance at the next time step is passed on to the controlled resistance in the simulation. The real time calculation of power is performed by a FORTRAN block. For the system shown in Fig. 9, using Thevenin's theorem, maximum power transfer from source towards load is calculated analytically by (32).

$$P_{\max} = \frac{E^2}{4 \times R_{load}} \tag{32}$$

This maximum power at bus 2 occurs when the magnitude of R_{load} equals the magnitude of the branch resistance (0.5 Ω). When power demand attains its maximum value, voltage at that particular bus reaches a value of $V_{critical}$. No further increase in power flow can occur. A reduction in load resistance causes the voltage to decrease sharply towards 0.

Variation of real power and voltage with respect to time is shown in Fig. 10. The green and red traces shown in this figure are power and voltage, respectively. Fig. 11 shows the corresponding P-V curve and the results are verified against the one published in [18].

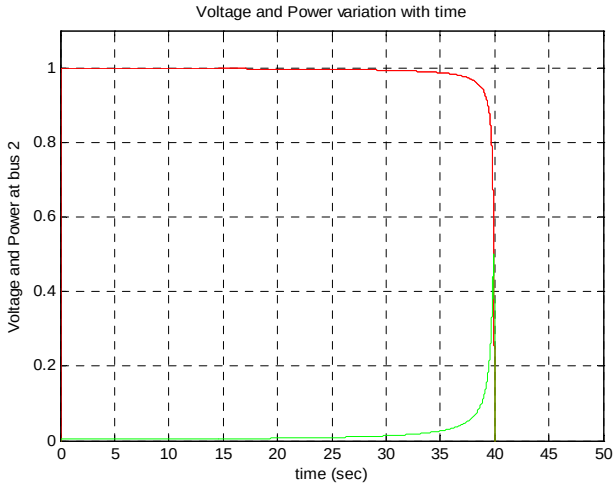

Fig. 10. Output from ATP model of DC system

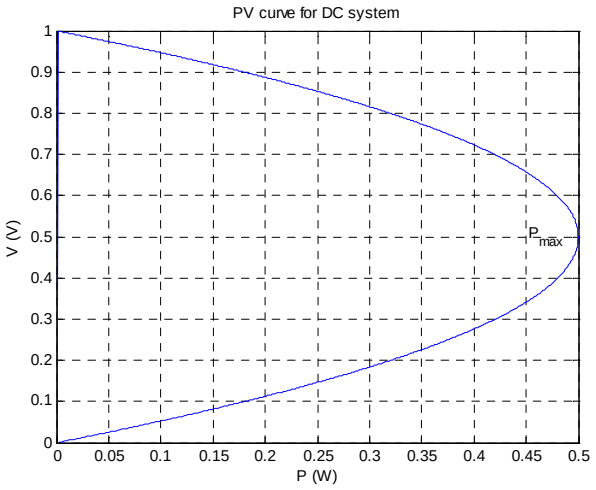

Fig. 11. P-V curve for DC system

V. Results and Analysis for AC Systems

A. Network Model

Different load models could be considered. Here we present the results for a unity power factor load and also a lagging load with the power factor of $pf = 0.8$. A 2 bus ac system as is shown in Fig. 12, is simulated to observe voltage and current waveforms and develop P-V curve to analyze voltage stability. The network is consisting of a generator and a load connected with a transmission line.

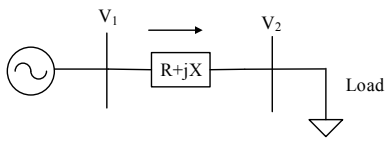

Fig. 12. 2 bus ac system

B. Resistive Load

The resistance (equivalent to a real power load) is varied according to (12) and the delivered power is calculated from the load voltage and current waveforms. Fig. 13 shows the load current and voltage waveforms. The green curve shows the current waveform and the red shows the voltage

waveform. As the value of resistance is decreased (The load increases) gradually, there is an increase in power demand and hence the load current increases. Also it is shown in this figure that the voltage and current waveforms are in phase; indicating a resistive load.

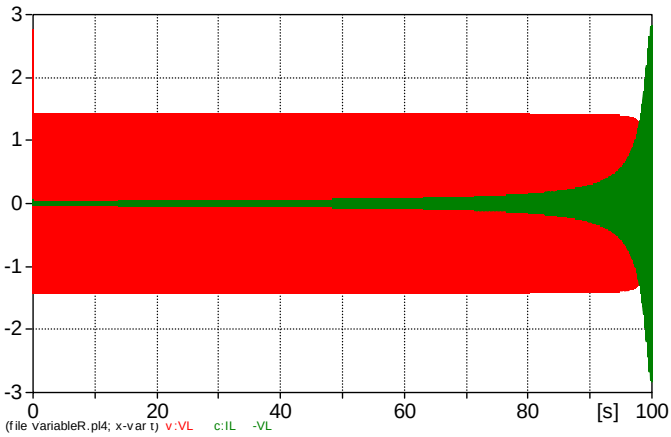

Fig. 13. Voltage and Current waveforms of an increasing resistive load

Fig. 14 shows the load power and voltage during simulation time as the load increases. It is clear based on this figure that before the collapse, the voltage remains almost constant as the load increases.

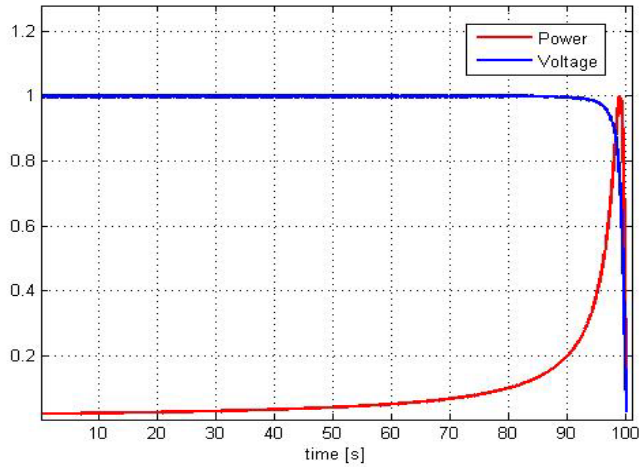

Fig. 14. Resistive load power and voltage

Fig. 15 shows the P-V curves obtained by both proposed simulation and the voltage equation given by equation (11). Both P-V curves are matching precisely. Since the load is purely resistive, $\theta = \cos^{-1}(1) = 0$ therefore, $\beta = \tan(0) = 0$. The red trace is the P-V curve developed from the proposed simulation and the blue trace is obtained by calculating the roots of the equation.

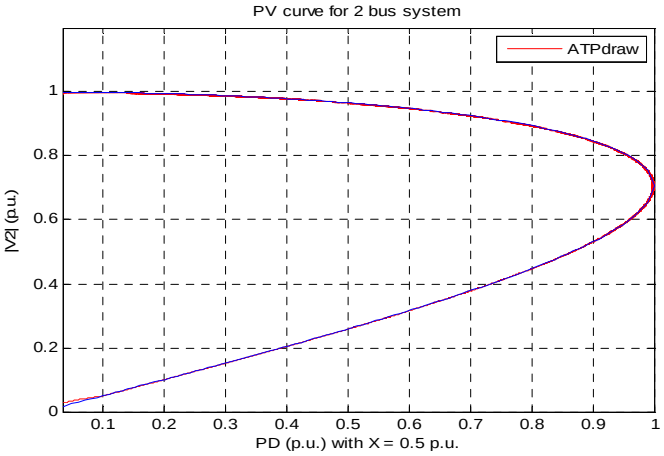

Fig. 15. P-V curves by time-domain method and mathematical equation

C. *Lagging Load*

In order to have a lagging load we combine the resistive load model in parallel with inductive load model. The model developed in ATPDraw is shown in Fig. 16. Using time-domain results, in each time step the load power and RMS values of voltage and current are calculated. To confirm that the load power factor remains constant, the phase angle difference between the voltage and current is also monitored. In each time step we increase the load and the voltage will ultimately collapse. This is shown in Fig. 17 in which the load power and RMS voltage are plotted in 100 seconds.

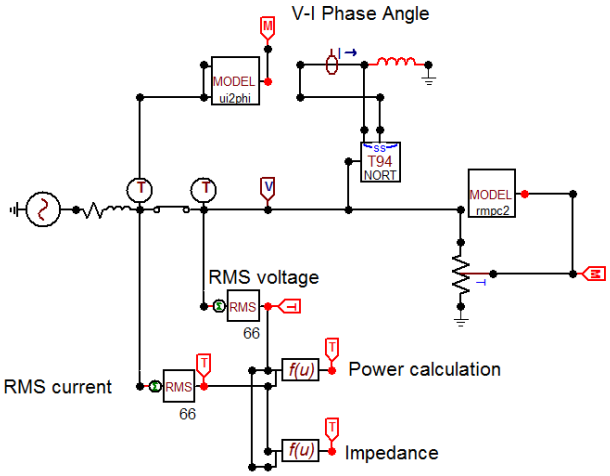

Fig. 16. Time-varying lagging load model

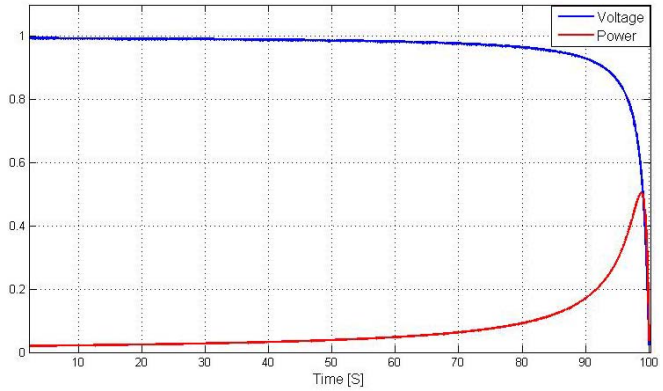

Fig. 17. Load power and voltage

Using time-domain method, we can develop the P-V curve which is being used to detect maximum system loadability and voltage stability. Fig. 18 shows the P-V curves developed for the 2 bus system for loads with different power factors using time-domain method.

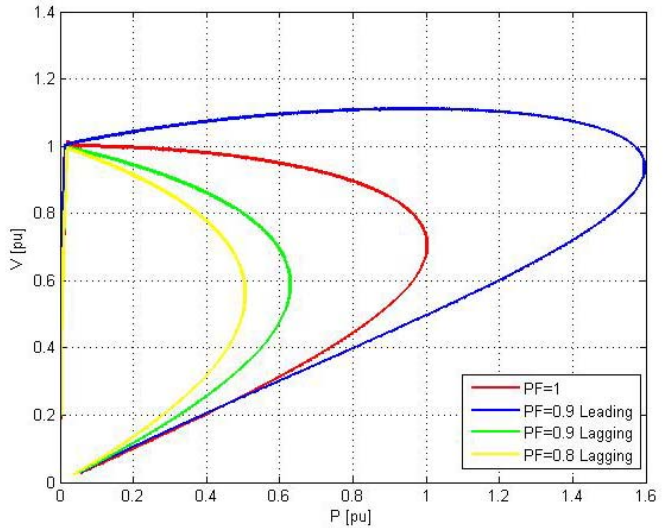

Fig. 18. P-V curve of loads with different power factors

VI. Time-Domain Method Verification

Fig. 15 showed that the P-V curves obtained by time-domain simulation and the power-voltage equation given by equation (11) precisely match. Now we will use Continuous Power Flow (CPF) method in order to verify the results of our proposed time-domain analysis method.

Fig. 19 shows the 2 bus system developed for this part. The detailed network data is shown in Table 1. Continuous power flow program is coded in Matlab. In each time step we increase the system load and conduct a power flow; voltage, current and the complex power are stored and after the simulation time they are used to plot the P-V curve. Fig. 20 shows the P-V curve obtained from CPF method and also the P-V curve obtained from time-domain method. As it is shown in this figure, the two plots match precisely. This means maximum power transfer point and voltage collapse could be precisely detected using time-domain method.

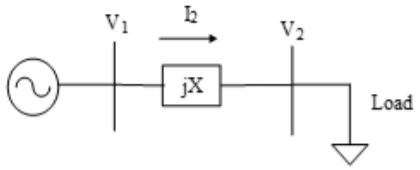

Fig. 19. 2 bus test system

TABLE I
Network Data

Generator Voltage	$1\angle 0$ V
Frequency	60 Hz
Transmission Line Inductance	1.326 mH
Initial Load	100 Ohm
Simulation Time	100 S

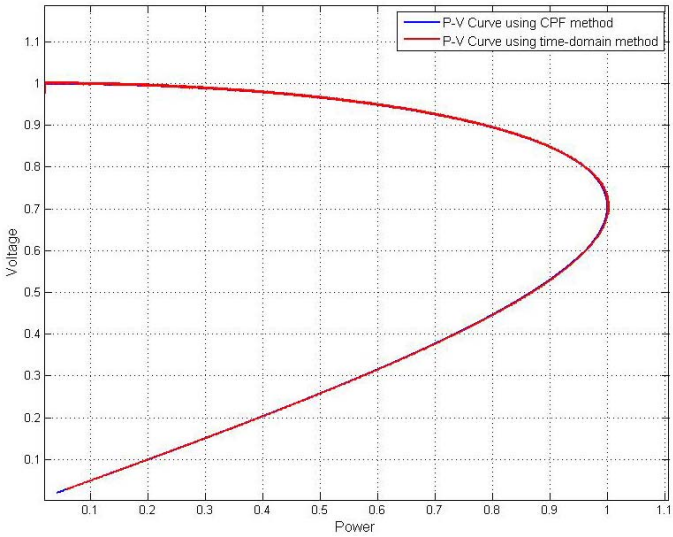

Fig. 20. P-V curves plotted using time-domain method and CPF

VII. Conclusion

This paper proposes a new approach for tracing P-V curve using the time-domain analysis. Most methods found in the literature use steady-state power-flow analysis for predicting voltage collapse; so the nonlinearity and frequency dependency of the system is not being considered. Simulation models proposed in this paper will help utilities to perform voltage collapse studies while including certain models for nonlinearities, transients and frequency dependent circuits. Power systems represented by these models are more realistic and accurate than their phasor counterparts.

Three different load models were developed in ATPDraw to simulate time-varying resistive, inductive and capacitive loads. Using these load models, any time-varying load with desired power factor can be simulated. To verify our results, the instantaneous time-domain simulation results are compared with continuous power flow method results which is used in steady-state voltage collapse analysis.

We have applied this method to 3-phase systems as well and the results precisely match with continuous power flow method. The presented method in this paper is the first step of an undergoing research and verifies the accuracy of time-

domain analysis method. Research is currently underway to develop a complete three phase model for voltage stability studies addressing nonlinearities relating to magnetic behavior and frequency dependency of different components and loads in power system. This simulation approach can also be used for educational purposes to help explain to student's the nature of voltage collapse.

REFERENCES

[1] P. Kundur, J. Paserba, V. Ajjarapu, G. Anderson, A. Bose, C. Canizares, N. Hatziargyriou, D. Hill, A. Stankovic, C. Taylor, T. Van Custem, and V. Vittal, "Definition and Classification of Power System Stability," *IEEE Trans. Power Syst.*, vol. 19, no. 2, pp. 1387–1401, 2004.

[2] Prabha Kundur, *Power System Stability And Control by Prabha Kundur*. McGraw-Hill, Inc.

[3] C. Rehtanz and J. Bertsch, "Wide Area Measurement and Protection System for Emergency Voltage Stability Control," in *Power Engineering Society Winter Meeting, IEEE*, 2002, vol. 00, no. c, pp. 842–847.

[4] M. Beiraghi and A. M. Ranjbar, "Online Voltage Security Assessment Based on Wide-Area Measurements," *IEEE Trans. POWER Deliv.*, vol. 28, no. 2, pp. 989–997, 2013.

[5] A. C. C. De Oliveira, D. M. Falc, G. N. T. Ý, G. L. Torres, and D. D. E. El, "Voltage Stability Assessment by Fast Time Domain Simulation and Interior-Point Optimal Power Flow," in *Power Systems Conference and Exposition, IEEE PES*, 2004.

[6] L.-A. Dessaint, I. Kamwa, and T. Zabaiou, "Preventive control approach for voltage stability improvement using voltage stability constrained optimal power flow based on static line voltage stability indices," *IET Gener. Transm. Distrib.*, vol. 8, no. 5, pp. 924–934, May 2014.

[7] Chandrabhan Sharma and Marcus G. Ganness, "Determination of the Applicability of using Modal Analysis for the Prediction of Voltage Stability", *IEEE/PES Transmission and Distribution Conference and Exposition*, pp. 1-7, March 2008.

[8] M. Hasani and M. Parniani, "Method of Combined Static and Dynamic Analysis of Voltage Collapse in Voltage Stability Assessment", *IEEE/PES Transmission and Distribution Conference \& Exhibition, Asia and Pacific*, pp. 1-6, April 2005.

[9] Robert J. Thomas and Anuchit Tiranuchit, "Dynamic Voltage Instability", *IEEE Proceedings of the 26th Conference on Decision and Control,* pp. 53-58, December 1987.

[10] Scott Greene, Ian Dobson, Fernando L. Alvarado, "Contingency Ranking for Voltage Collapse via Sensitivities from a Single Nose Curve", *IEEE Transactions on Power Systems*, Vol. 14, No. 1, pp. 232-240, February 1999.

[11] Abhyankar S. G, Fluek A.J, "Simulating voltage collapse dynamics for constant power systems with constant power load models", *IEEE Power and Energy Society General Meeting*, 2008, pp. 1-6.

[12] Abhyankar S.G, Flueck A. J, "A new confirmation of voltage collapse via instantaneous time domain simulation", *North American Symposium*, 2009, pp. 1-6.

[13] B.A. Mork, "Five-Legged Wound-Core Transformer Model: Derivation, Parameters, Implementation and Evaluation", IEEE Trans. Power Delivery, vol. 14, no. 4, pp. 1519-1526, October 1999.

[14] L. Dubé and B.A. Mork, "Variable Capacitance and Inductance in ATP", EMTP News, Leuven, Belgium, vol. 5, no. 1, pp. 33-36, March 1992.

[15] C. W. Taylor, "Power System Voltage Stability", McGraw-Hill, 1994.

[16] László Prikler and Hans Kristian Høidalen, "ATPDrarw Version 5.6 for Windows 9x/NT/2000/X/Vista - Users!` Manual", November 2009.

[17] Laurent Dubé, "USER GUIDE TO MODELS IN ATP", November 1996.

[18] Thierry Van Cutsem, Costas Vournas, "Voltage Stability of Electric Power Systems", KAP, 1998.